Available online at www.sciencedirect.com

ScienceDirect

Procedia Engineering 173 (2017) 314 – 322

Procedia Engineering

www.elsevier.com/locate/procedia

11th International Symposium on Plasticity and Impact Mechanics, Implast 2016

Finite Element Analysis of Laminated Composite Skewed Hypar Shell Roof Under Oblique Impact with Friction

Sanjoy Das Neogi[a,*], AmitKarmakar[b], DipankarChakravorty[c]

a. Civil Engineering Department, MeghnadSaha Institute of Technology, Kolkata-700150, India

b. Mechanical Engineering Department, Jadavpur University, Kolkata-700032, India

c. Civil Engineering Department, Jadavpur University, Kolkata-700032, India

Abstract

Impact of foreign objects on laminated composite has become a great concern despite its other advantages. Hypar (hyperbolic-paraboloid),a preferred shell roof geometry is frequently subjectedto such impacts. In most of the practical situations such impacts are oblique. Present study investigates dynamic behaviour of a simply supported composite hypar shell roofs under oblique impact, considering modified Hertzian contact law, for different impact velocities and impact angles allowing for anisotropic friction. Time dependent equations are solved using Newmark's time integration algorithm. Time histories of contact force at point of impact and that of displacement are presented to extract significant engineering conclusions. There are also proposals of practical parameters for designing such shells through static simplification of the problems.

© 2017 The Authors. Published by Elsevier Ltd. This is an open access article under the CC BY-NC-ND license (http://creativecommons.org/licenses/by-nc-nd/4.0/).

Peer-review under responsibility of the organizing committee of Implast 2016

Keywords:Composite, hypar shell, finite element, low velocity, oblique impact, friction

1. Introduction

Composites are engineered materials and are preferred in several sectors of industry for their high specific stiffness, strength, low specific weight and corrosion resistance.

Nomenclature

a, b	length and width of shell in plan.
C	rise of hypar shell.
D	flexural rigidity of shell
E_{11},E_{22}	elastic moduli
G_{12}, G_{13}, G_{23}	shear moduli of a lamina with respect to 1, 2 and 3 axes of fibre
h	shell thickness

* Corresponding author. Tel.: +91 9831532846 ;*E-mail address:*sanjoy_civil08@yahoo.com: sanjoycivil08@gmail .com

1877-7058 © 2017 The Authors. Published by Elsevier Ltd. This is an open access article under the CC BY-NC-ND license (http://creativecommons.org/licenses/by-nc-nd/4.0/).

Peer-review under responsibility of the organizing committee of Implast 2016

doi:10.1016/j.proeng.2016.12.023

N_i	shape function of i^{th} node
R_{xy}	radius of cross curvature of shell
u, v, w	translational degrees of freedom at each node of shell element
z_k	depth of k^{th} layer of laminate measured from neutral axis
α, β	rotational degrees of freedom at each node of shell element
ρ	density of material
θ_i	angle of impact made with vertical axis
μ_x, μ_y	coefficient of friction between target and indenter in global x- and y-direction

In the face of these advantages impact-induced damage, due to low transverse shear capacity of laminated composites, has become a great disquiet. Civil engineering shell roofs, might frequently be exposed to such impact due to wind born debris or snowfall.

The classical contact law between isotropic elastic solids derived by Hertz [1] was found to be inadequate for composite materials. Yang and Sun [2] proposed a power law framed on static indentation tests. The modified version of the same was further proposed by Tan and Sun [3].

Impact response of simply supported initially stressed plate was reported by Sun and Chen [4] using modified contact law [3].Toh et al. [5] studied impact analysis of an orthotropic laminated cylindrical shell under low-velocity impact. Shim et al.[6] reported the elastic response of glass/epoxy laminated composite ogival shell subjected to low velocity impact using bi-harmonic polynomial solution. A numerical solution was proposed by Chun and Lam [7] for analysing a laminated composite plate under low-velocity impact. In all these studies oblique impact related research remained untouched.

In most of the practical situations impact is oblique. Sliding of such impactor over the target surface may cause a frictional drag. Dry friction has been considered conventionally dependent on normal pressure of contact but nearly independent of sliding speed. Conversely, Bijwe et al. [8] performed an analysis on the lubricated sliding of metals on polymers for different speeds and temperatures, indicating a correlation between the frictional behavior of the materials. Friction depends on the track of sliding, frictional anisotropy results from anisotropic surface irregularity.Theanisotropy of such mechanical properties appears essentially in laminated composites. Zmitrowicz [9] proposed linear and non-linear models of anistropic dry friction with respect to principal directions of friction and friction symmetries. Brach [10] and Sundarajan [11] confirmed that the coefficient of friction varies with the strain built up in the near-surface contact region of the target material as a function of incident angle and incident velocity. A finite element solution was studied by Sachdeva and Ramakrishnan [12] for two-dimensional elastic contact problems with friction. Tu and Chao [13] worked out the contact behavior of a simply supported plate considering anisotropic friction.

A look through the literature reveals the fact that impact response of civil engineering shell structures has not received due attention. A parallel review reveals that the hypar shell was studied recently by Sahoo and Chakravorty[14] for free vibration issues only. The single report on impact response of composite hypar shell was due to Das Neogi et al [15] where in, only normal impact problem was studied. Hence, this paper aims to carry out a study onlow velocity oblique impact. Dry friction is considered depending on normal pressure between contacts.

2. Mathematical form

is a thin, shallow, doubly curved, anticlastic skewed hypar shell (Fig.-1)of laminated composite and linearly elastic material having cross curvature $1/R_{xy}$, with uniform thickness *h*. A shell is characterized as shallow if any infinitesimal line element of its middle surface is approximated by the length of its projection on the *XY* plane. This implies that

$$\left(\frac{\partial z}{\partial x}\right)^2 << 1 \qquad \left(\frac{\partial z}{\partial y}\right)^2 << 1 \qquad \left(\frac{\partial z}{\partial x}\right)\left(\frac{\partial z}{\partial y}\right) << 1 \tag{1}$$

Similarly, the lateral boundary of a shallow shell is also estimated by its projection on the *XY* plane with accordance to its boundary conditions. According to Vlasov [16], the above conditions are practically satisfied for shells with a rise to span ratio less than 1/5 and cross curvature is approximately represented as: $\frac{1}{R_{xy}} = \frac{\partial^2 z}{\partial x \partial y}$ (2)

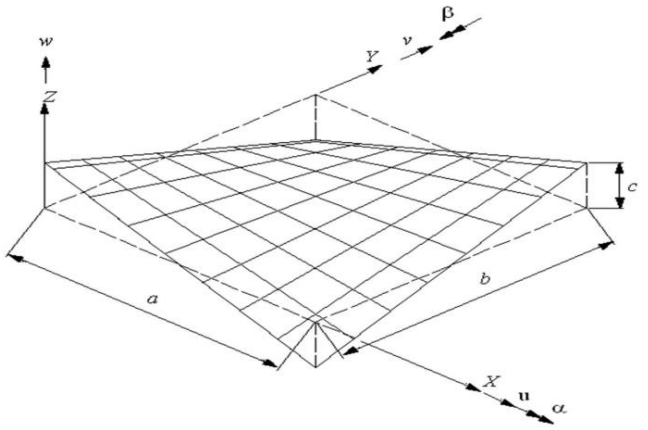

Surface equation: $z = \frac{4c}{ab}\left(x - \frac{a}{2}\right)\left(y - \frac{b}{2}\right)$

Figure-1 Surface of a skewed hypar shell and degrees of freedom

An eight-noded curved quadratic isoparametric finite element is used for analysis with five degrees of freedom at each node (Fig-1). The generalised displacement vector of an element is expressed in terms of the shape functions and nodal degrees of freedom as:

$$[u] = [N]\{d_e\} \tag{3}$$

(4)

The element stiffness and mass matrices are derived by using the minimum energy principle. The element stiffness matrix is

$$[K] = \iint [B]^T [D][B] dx dy \tag{5}$$

Incorporating both the translatory and rotatory inertia terms, the generalised inertia matrix takes the following form

$$[M\ ] = \iint [N]^T [\rho][N] dx dy \tag{6}$$

The dynamic equilibrium equation of the target shell for low velocity impact is given by the following equation:

$$[M]\{\ddot{\delta}\} + [K]\{\delta\} = \{F\} \tag{7}$$

where [M] and [K] are global mass and elastic stiffness matrices, respectively.{δ} is the global displacement vector. For the impact force vector {F}, the force vector is given as

$$\{F\} = \{0\ 0\ 0\ \ldots . F_C \ldots\ldots 0\ 0\ 0\}^T \tag{8}$$

Here F_C is the contact force given by the indentation law and the equation of motion of the rigid impactor is given as

$$m_i \ddot{\omega}_i + F_C = 0 \tag{9}$$

where m_i and $\ddot{\omega}_i$ are the mass and acceleration of the impactor respectively.

The contact force model following Sun and Chen [4] has been incorporated in the present finite element formulation with appropriate modification for friction generated due to oblique impact. If k is the contact stiffness and α_m is the maximum local indentation, the contact force F_c during loading is given by

$F_c = k\alpha_i^{1.5} 0 < \alpha_i \leq \alpha_m$ (10)

The indentation parameter α_i at any i[th] iteration depends on the difference of the displacements of the impactor and the target structure at any instant of time, and the contact force as well i.e. the values of $\alpha_i$keepschanging with time on account of time-varying displacements of both the rigid impactor and the target structure. In the present analysis where oblique impact is under consideration, effect of friction generated due to sliding of the impactor over the surface of the target structure has been considered along with the vertical disarticulation while calculating the indentation parameter and the contact force at each time step. Considering displacements along any arbitrary global directions for oblique impact, the indentation α_i at any i[th] iteration is given as

$\alpha_i = w_i(t)\cos\theta_i - w_s(x_c, y_c, t_c)$ (11)

Where w_i and w_s are displacement of impactor and target shell along any arbitrary direction (θ_i) at the point of contact (x_c ,y_c) and at any time instant (t_c), respectively.

Thus with the maximum indentation taking place, the maximum contact force is attained, followed by the displacement of the impactor reaching its maximum. Subsequently, the displacement of the impactor gradually decreases, but the target point displacement keeps on changing and finally increases to a maximum and there comes a time when these two displacements become equal . This leads to zero value of indentation. Eventually the contact force becomes zero when the impactor loses the contact with the target. This process of attaining the maximum contact force till the declining of the same to zero is fundamentally referred to as unloading. Provided that the mass of the impactor is not very small, a second impact may occur upon the rebound of the target structure leading to an identical phenomenon of contact deformation and attainment of the maximum. This is known as reloading. If F_m is the maximum contact force at the onset of unloading and α_m is the maximum indentation during loading, the contact force F_c for unloading and reloading are expressed as [4].

Unloading phase: $F_c = F_m \left[\frac{\alpha_i - \alpha_0}{\alpha_m - \alpha_0}\right]^{2.5}$ (12)

Reloading phase: $F_c = F_m \left[\frac{\alpha_i - \alpha_0}{\alpha_m - \alpha_0}\right]^{1.5}$ (13)

$F_{cz(i+1)} = F_{cz(i)}(t)\cos\theta_i$ (14)

$F_{cx(i+1)} = F_{cx(i)}(t)\sin\theta_i - \mu_x F_{cx(i)}(t)\cos\theta_i$ (15)

$F_{cy(i+1)} = F_{cy(i)}(t)\sin\theta_i - \mu_y F_{cy(i)}(t)\cos\theta_i$ (16)

Where μ_x, μ_y are the coefficient of friction in global x and y-direction of graphite-epoxy composite, whereas θ_i is the angle of impact with z-direction. $F_{cki}$is the contact force in k[th] direction at i[th] iteration. The solution for the equations of motion given by Equations (1) and (3) is solved using Newmark constant-acceleration time integration algorithm in the present analysis. Equation (1) may be expressed in iteration form at each time step.

$$\left[\bar{K}\right]\{\Delta\}_{t+\Delta t}^{i+1} = \frac{\Delta t^2}{4}\{F\}_{t+\Delta t}^{i} + [M]\{b\}_i \quad (17)$$

Where

$$\left[\bar{K}\right] = \frac{\Delta t^2}{4}[K] + [M] \quad (18)$$

$$\{b\}_t = \{\Delta\}_t + \Delta t\left\{\dot{\Delta}\right\}_t + \frac{\Delta t^2}{4}\left\{\ddot{\Delta}\right\}_t \quad (19)$$

The same solution scheme is also utilized for solving the equation of motion of the impactor, i.e. Equation (7). It is to be noted that a modified contact force $F_{t+\Delta t}^{i}$ obtained from the previous iteration is used to solve the current response $\{\Delta\}_{t+\Delta t}^{i+1}$. The iteration procedure is continued until the equilibrium criterion is met.

3. Numerical examples

Problems are solved in this paper to validate the present finite element code and to numerically explore the different behavioral aspects of composite skewed hypar shell roof under low-velocity impact with an obliquity. Firstly the present formulation is applied to solve natural frequencies of graphite-epoxy twisted plates which are structurally similar to skewed hypar shells. This problem is expected to validate both the stiffness and mass matrix formulation

of present finite element code comparing with the published one [17]. Another problem of impact response of composite plate, solved earlier by Tu and Chow [13] serves as the benchmark to validate the correct incorporation of oblique impact formulation considering the effect of friction for simply-supported boundary condition.The details of the benchmark problems are furnished along with Table-1, Fig-2.

Table 1 Non dimensional natural frequencies (ϖ) for three layer graphite epoxy twisted plates $[\theta/-\theta/\theta]$

Angle of twist θ **(deg)**	**0^0**	**15^0**	**30^0**	**45^0**	**60^0**	**75^0**	**90^0**
$\phi = 15^\circ$ Qatu and Lessia[17]	1.0035	0.9296	0.7465	0.5286	0.3545	0.2723	0.2555
Present formulation	0.9990	0.9257	0.7445	0.5279	0.3542	0.2720	0.2551
$\phi = 30^\circ$ Qatu and Lessia[17]	0.9566	0.8914	0.7205	0.5149	0.3443	0.2606	0.2436
Present formulation	0.9490	0.8842	0.7181	0.5142	0.3447	0.2613	0.2444

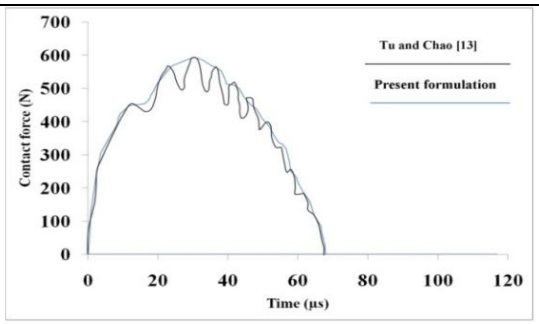

E_1=128 GPa. E_2=E_3=8 GPa. G_{12}=G_{13}=4.5 GPa. G_{23}=1.6 GPa. ν_{12}=ν_{23}=ν_{31}= 0.28,
γ =1515 kg/m^3, μ_1 =0.2, μ_2 =0.4, a =150 mm b =150 mm, h =9.95 mm, Ds =25.4 mm
ms= 0.125kg, v_x= 20.0 m/s v_z= 5.0 m/s

Figure-2 Contact force history of a simply supported plate under oblique impact

Besides the aforementioned problems, responses of skewed hypar shells being impacted at the central point are also studied for eight different shell options combining two boundary conditions and four laminations. Six impact velocities with four different angle of impact are considered. The details of the authors' own problems are furnished below.

i) Boundary conditions — Simply-supported (SS)
ii) Laminations — +45˚/-45˚ (Angle ply or AP)0˚/90˚ (Cross ply or CP)
iii) Velocityof impact (m/s)[2] — 1, 2, 3, 5, 7, 10
iv) Angle of impact (θ_i) — 0^0, 15^0, 30^0, 45^0
iv) Details of shell geometry — a = 1.0m, b =1.0m, t=0.02m, c=0.2m

4. Results and discussions

4.1. Results of benchmark problems

Table-1 and Fig-2 furnish the results of the benchmark problems including the published ones and those obtained by the present approach. The fundamental frequencies of the composite twisted plate as obtained here closely match with those reported by Qatu and Lessia [17] and hence the correct incorporation of the stiffness and mass matrices of composite twisted plate, which are geometrically analogous to skewed hypar shells, in the present code, is established. The contact force history obtained by the present approach for a simply-supported composite plate

under oblique impact considering the effect of friction shows a good agreement with that reported by Tu and Chao [13]. This confirms the correct incorporation of the oblique impact formulation considering the effect of friction for simply-supported boundary condition in the present finite element code. Here the authors have taken the liberty of converting the hypar shell formulation to plate by putting the value of c (Fig-1) equal to zero.

4.2. General behaviour of the hypar shells under oblique impact

The finite element mesh implemented in the present study is based primarily on force and displacement convergence criteria. All the results of contact force and displacement that are presented are arrived at only after the study of time step convergence.

Table 2 and 3 contains the maximum values of the contact force, maximum dynamic displacement for different impact velocities and different angle of impact for simply-supported boundary condition. The values of equivalent static loads and dynamic magnification factors (as explained hereafter) are also furnished in the tables.

Displacement histories are studied on the central point where the impactor strikes the shell. Typical time histories of contact force and displacement for simply-supported shell are shown in Fig-3 and Fig-4 for different impact angle and for impact velocity of 10m/s only.

While studying low velocity impact response, struck by the spherical impactor centrally, it is observed that the contact force follows a parabolic variation having a single peak. After some time, which in each of these cases is around or less than 60μs, the contact force converges to zero value for normal impact whereas, the oblique impact dies down at about 35μs. It is interesting to note that higher the impact velocity, higher is the contact force, but the force dies down to zero relatively faster (although such pictorial representation is not furnished here to maintain brevity). This behavior may be attributed to the rapid elastic rebound of the impactor with the increment in the velocity value followed by detachment which causes contact force to decay out. It is also worth noting that the time instants corresponding to peak contact forces and peak displacements at the centre point do not match. This is because the resultant displacement at any time instant is a cumulative effect of the instantaneous contact force value and the inertia effect of the previous instant. The figures showing the transient displacement show that vibration continues even after the force dies down with successively occurring peaks, though the peak values are less in magnitude than the highest peak which occurs a bit after the instant of maximum contact force but before the full decay. It is to be noted that the contact forces and the transient displacements do not exhibit any tendency of local reversal. The peak transverse contact force in oblique impact is considerably low than normal impact as component of the impact is shared in tangential direction. Contact force decreases as the obliquity increases.

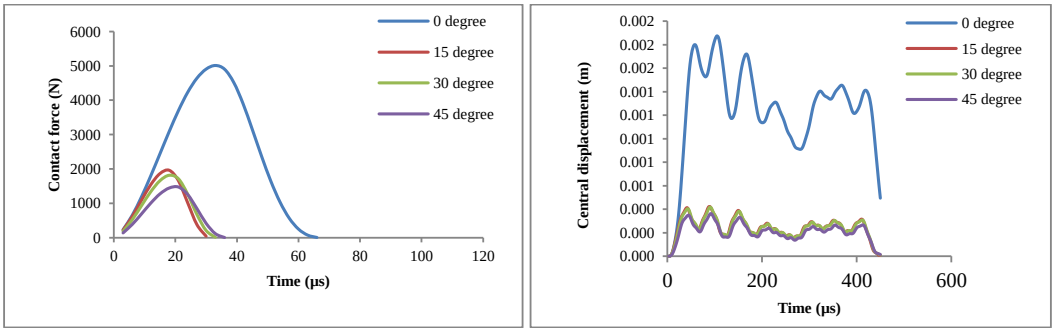

Figure- 3 Impact response of simply supported anti-symmetric angle ply (SS/AS/AP) compositehypar shells for impact velocity 10m/s

4.3. Equivalent Static Load and Dynamic Magnification Factor

To estimate the equivalent static load (ESL) corresponding to a particular impact velocity , a concentrated load at the centre (point of impact) is applied and adjusted the yield a central displacement equal to the maximum dynamic displacement. It is further explored to estimate the magnitude of the central displacement when the peak

contactforce is applied at the point of impact as a static concentrated load. The central displacement obtained under such a load when divides the maximum dynamic displacements yields dynamic magnification factor (DMF).The variations of maximum contact force, maximum dynamic displacement and equivalent static load (ESL) with impact velocity are almost linear and are increasing functions of impact velocity. However the dynamic magnification factor (DMF) and the impact velocity shows a logarithmicdetrimental relation with impact velocity. This enables the designer to practice the static approximation of the problem.

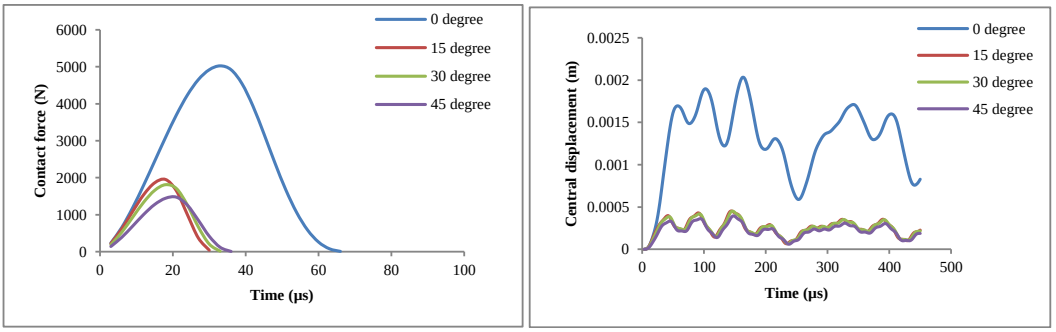

Figure- 4 Impact response of simply supported cross ply (SS/AS/CP) composite hypar shells for impact velocity 10m/s

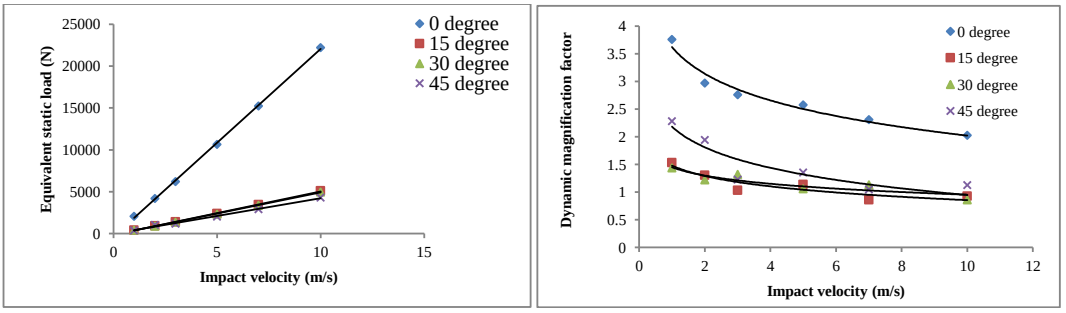

Figure-5 Variation of maximum impact load, maximum displacement, equivalent static loadanddynamic magnification factor with velocity for simply supported anti-symmetric angle ply (SS/AS/AP) composite hypar shells

Velocity (m/s)	Maximum contact force (N)				Maximum displacement (m)				Equivalent static load (N) ESL				Dynamic magnification factor			
	0^0	15^0	30^0	45^0	0^0	15^0	30^0	45^0	0^0	15^0	30^0	45^0	0^0	15^0	30^0	45^0
1	309.3	112.8	104.7	86.0	0.00017	0.00003	0.00003	0.00003	2074	427.2	421.0	364.2	3.76	1.533	1.440	2.283
2	713.6	265.6	246.7	276.7	0.00034	0.00007	0.00007	0.00008	4206	911.1	895.1	1030.9	2.97	1.306	1.226	1.9428
3	1165.9	436.5	406.6	332.2	0.00050	0.00011	0.00011	0.00010	6204.7	1407.4	1382.7	1200	2.76	1.035	1.322	1.227
5	2162.3	822.4	770.2	622.8	0.00086	0.00019	0.00019	0.00016	10638.4	2395.1	2333.3	2012.3	2.58	1.14	1.061	1.355
7	3252.5	1255.2	1161.6	951.4	0.00123	0.00028	0.00027	0.00024	15237.4	3444.4	3382.7	2913.6	2.31	0.863	1.137	1`.052
10	5010.8	1961.3	1815.5	1473.7	0.00180	0.00041	0.00040	0.00035	22207.5	5098.8	4975.3	4308.6	2.03	0.93	0.864	1.131

Table 2 Maximum contact force, maximum dynamic displacement, equivalent static load, dynamic magnification factor for different velocities of the impactor for simply supportedanti-symmetricangle ply (SS/AS/AP) hypar shell

Velocity (m/s)	Maximum contact force (N)				Maximum displacement (m)				Equivalent static load (N) ESL				Dynamic magnification factor			
	0^0	15^0	30^0	45^0	0^0	15^0	30^0	45^0	0^0	15^0	30^0	45^0	0^0	15^0	30^0	45^0
1	309.3	112.8	104.7	86.0	0.00017	0.00003	0.00003	0.00003	2074	427.2	421.0	364.2	3.76	1.533	1.440	2.283
2	713.6	265.6	246.7	276.7	0.00034	0.00007	0.00007	0.00008	4206	911.1	895.1	1030.9	2.97	1.306	1.226	1.9428
3	1165.9	436.5	406.6	332.2	0.00050	0.00011	0.00011	0.00010	6204.7	1407.4	1382.7	1200	2.76	1.035	1.322	1.227
5	2162.3	822.4	770.2	622.8	0.00086	0.00019	0.00019	0.00016	10638.4	2395.1	2333.3	2012.3	2.58	1.14	1.061	1.355
7	3252.5	1255.2	1161.6	951.4	0.00123	0.00028	0.00027	0.00024	15237.4	3444.4	3382.7	2913.6	2.31	0.863	1.137	1`.052
10	5010.8	1961.3	1815.5	1473.7	0.00180	0.00041	0.00040	0.00035	22207.5	5098.8	4975.3	4308.6	2.03	0.93	0.864	1.131

Table 3 Maximum contact force, maximum dynamic displacement, equivalent static load, dynamic magnification factor for different velocitiesof the impactor for simply supported anti-symmetric cross ply (SS/AS/CP) hypar shell

4.4. Comparative performance of angle ply and cross ply shell

The behavior of the impact response of simply supported cross(SS/CP) and angle ply(SS/AP) shell may be studied through Fig.3 and 4 and Table-2 and 3. The nature of contact force and dynamic displacement for this class (SS/ CP) of shell is more or less similar to what is discussed before for SS/AP shell. One interesting difference is that for SS/ CP shell the peak dynamic displacement does not only show a phase lag with respect to the peak contact force but by the time displacement value reaches the peak, the contact force value dies down totally. This shows that the after-effect of impact are some times more severe than the shell response during the impact and study of displacement variation even after the contact force decays to a null value is absolutely necessary. However, after passage of some more time the subsequent local maxima which are obtained do not touch the peak.
The dependence of the maximum contact force, the peak dynamic displacement and the equivalent static load (ESL) on the impactor velocity in case of simply supported cross ply (SS /CP) shell are similar to what is observed in case of simply supported angle ply (SS/AP) shell.

5. Reference

[1] H.Hertz, On the contact of elastic solids. *Journal fur die reine und angewandteMathematik*, 92 (1881) 156-171.

[2] S.H. Yang, C.T.Sun, Indentation law for composite laminates, *Compos. Mat.: Testing and Desig., ASTME STP* 787 (1985) 425-446.

[3] T.M.Tan, C.T. Sun, Use of statical indentation laws in the impact analysis of laminated composite plate, *J. Appl. Mech.* 52 (1983) 6-12.

[4] C.T. Sun, J.K. Chen, On the impact of initially stressed laminates, *J. Compos. Mat.* 19 (1985) 490-503.

[5] S.L. Toh, S.W. Gong, V.P.W.Shim, Transient stress generated by low velocity impact on orthotropic laminated cylindrical shell, *Compos. Struct.* 31(3) (1995) 213-228.

[6] V.P.W. Shim, S.L. Toh, S.W.Gong, The elastic impact response of glass/epoxy laminated ogival shells, *Int. J. Impt. Engg.* 18(6) (1996) 633-655.

[7] L. U. Chun , K. Y. Lam, Dynamic response of fully-clamped laminated composite plates subjected to low-velocity impact of a mass, *Int. J. Solids Struc.*, 35 (11) (1998) 963–979.

[8] Bijwe J, Tewari US, Vasudevan P. Friction and wear studies of polymer composite material. Wear, 138(1) (1990) 61–76.

[9] Zmitrowicz A. Mathematical descriptions of anisotropic friction. *Int J Solids Struct*, 25(8) (1989) 837–862.

[10] Brach RM. Impact dynamics with applications to solid particle erosion. *Int J Impt. Eng.* 7(1) (1988) 37–53.

[11] Sundararajan G. The energy absorbed during the oblique impact of a hard ball against ductile target materials. *Int J Impt. Eng*. 9(3) (1990) 343–358.

[12] Sachdeva TD, Ramakrishnan CV. A finite element solution for the two-dimensional elastic contact problems with friction. *Int J NumerMetho. Eng*,17(8) (1981)1257–1271.

[13] C.Y. Tu, C.C. Chao, Three-dimensional contact dynamics of laminated plates: Part 2. Oblique impact with friction, Compo. Part-B: Eng. 30 (1999) 23–41.

[14] S. Sahoo, D. Chakravorty, Finite element bending 9ehavior of composite hyperbolic paraboloidal shells with various edge conditions, *J. Strain Analysis for Engg. Design*, 39 (5) (2004) 499-513.

[15] S.DasNeogi, A. Karmakar, D. Chakravorty, Impact response of simply supported skewed hypar shell roofs by finite element, *J ReiforcedPlactics Compos.*30(21) (2011) ,1795-1805.

[16] V.Z. Vlasov, "AllegemeineSchalentheorie und ihreanwendung in dartechnik", Akademie-VerlagGmBH, Berlin 1958

[17] Qatu, M. S. and Leissa, A. W., "Natural frequencies for cantilevered doubly-curved laminated composite shallow shells", Computers and Structures. 17(3), 227-256, (1991)